Characterization of corrosion products in the permeable reactive barriers

Y. Roh · S.Y. Lee · M.P. Elless

Abstract The impact of geochemical processes and microbial activity has been a major concern for the long-term performance of reactive iron barriers because corrosion products and precipitates during the water treatment with reactive materials will decrease the reactivity and permeability of the iron bed. This study characterizes corrosion products in reactive iron barrier as well as evaluates the effect of the iron corrosion products and precipitates on iron wall performance during contaminated-water treatment under varying conditions. Major phases in the reactive iron barrier include iron oxides, carbonates, iron sulfides, and elemental sulfur, depending on the degree of iron oxidation, groundwater chemistry, and microbial activity. Detailed geochemical and mineralogical characteristics are imperative for long-range predictions of the reactive iron wall performance on water treatment because the surface coating materials reduce the effectiveness of the zero-valent iron media.

Keywords Groundwater treatment · Iron oxides · Trichloroethene · Uranium · Zero-valent iron

Introduction

Many US Department of Energy sites have problems associated with wastewater and groundwater plumes containing unacceptable levels of radionuclides (e.g. ^{99}Tc, ^{235,238}U) and chlorinated organic compounds (COCs) such as trichloroethene (TCE), trichloroethane (TCA), and dichloroethene (DCE) isomers. A commonly-used method for remediating groundwater contaminated with COCs is called "the pump-and-treat technology", which pumps water from the ground and treats it ex situ. After pumping, conventional separation technologies for removing uranyl carbonate complexes and the pertechnetate anion include anion exchange resins or coprecipitation by ferrous sulfate and sodium hydroxide treatment (Lee and Bondietti 1983). However, such chemical treatment not only generates secondary wastes but also leaves chemicals (Na^+, SO_4^{2-}) in the treated waters.

Use of barriers filled with reactive media such as zero-valent metals to clean contaminant plumes is an emerging technology for in situ and ex situ remediation of contaminated groundwaters (Matheson and Tratnyek 1994). The reactive media degrade, sorb, or precipitate chlorinated solvents, metals, radionuclides, and other pollutants as the contaminant plume flows through the treatment wall. Zero-valent iron (Fe^0) is the leading treatment medium to dechlorinate halogenated hydrocarbons (Gillham and O'Hanneisin 1994; Orth and Gillham 1996; Liang and others 1997; Roh and others 2000a), and to precipitate heavy metals (Powell and others 1995) and radionuclides (Cantrell and others 1995; Roh and others 1996; Roh and others 2000b). Other media that can be used in treatment walls include zeolites and activated carbon, which sorb and entrap contaminants on the barrier surface, and limestone, which neutralizes acidic, lead-contaminated groundwater and traps lead in the barrier (Morrison and Spangler 1993; Haggerty and Bowman 1994; Environmental Protection Agency 1996).

Several types of geochemical reactions, such as iron corrosion, redox reactions, sorption, and precipitation, can occur in this reactive permeable wall. The geochemical changes in reactive media, depending upon the inorganic characteristics of the water, can result in the formation of iron oxides, carbonate minerals, and other solid phases. Precipitates formed within the reactive media can, over time, fill the pore spaces, thereby reducing the permeability. Precipitates also adhere to the Fe^0 surfaces, blocking the reaction sites and thus reducing the reactivity of the Fe^0. This study characterizes corrosion products in a reactive Fe^0 barrier under varying conditions such as groundwater chemistry (i.e. alkalinity, pH, etc.) and types of contaminants in the field and laboratory.

Received: 17 September 1999 · Accepted: 11 April 2000

Y. Roh (✉) · S.Y. Lee
Environmental Sciences Division,
Oak Ridge National Laboratory, Oak Ridge,
Tennessee 37831-6038, USA
e-mail: rohy@ornl.gov
Tel: 423-576-9931
Fax: 423-576-8646

M.P. Elless
Edenspace Systems Corporation, Reston, Virginia 20191, USA

Materials and methods

Materials used as a reactive media

Reactive media used for TCE dechlorination and uranium immobilization in the laboratory were mineralogically characterized, and geochemical changes in the influent and effluent waters were determined. Three separate boro-silicate glass columns (2.0-cm diameter and 35-cm long) were filled with 10-cm long Cercona Fe^0 foam, Master Builder Fe^0 filings, and Peerless Fe^0 filings. Direct current (30 V, 0.05 A) and without direct current application were also used to treat groundwater contaminated with radionuclides and TCE. The direct current applied on the iron-based reactive wall controls the oxidation rate of the iron as electrons transverse an external circuit to a Fe^0 cathode, where they engage in reductive immobilization of radionuclides and reductive TCE dechlorination (Roh and others 2000a,b).

Effluent waters and reactive media used at two sites, the X-625 groundwater treatment facility at the Portsmouth Gaseous Diffusion Plant in Portsmouth, Ohio and the Y-12 Plant in Oak Ridge, Tennessee, were characterized for field study. The X625 groundwater facility was constructed to evaluate ex situ reactive iron barriers with Master Builder or Peerless iron filing for remediating TCE-contaminated groundwater (Liang and others 1997). In addition, the Bear Creek Valley treatability study at the Y-12 site in Oak Ridge was designed to remediate radionuclide-contaminated groundwater using ex situ reactive iron barrier walls with Master Builder or Peerless iron filings (Science Applications International Corporations 1998).

The characteristics of the reactive Fe^0 barrier media used for the laboratory and field study are summarized in Table 1. These Fe^0 media are inexpensive and the most used materials that have shown encouraging results in removing contaminants from groundwater (Matheson and Tratnyek 1994; Liang and others 1997; Roh and others 2000a,b).

Geochemical and mineralogical characterization

The chemical parameters of the influent water for the two field studies are summarized in Table 2 (Liang and others 1997; Science Applications International Corporations 1998). The major aqueous components of radionuclide-contaminated water from the Y-12 site are bicarbonate, sulfate, and calcium (Ca), which reflect inputs from the underlying carbonate strata of the contaminated site, S-3 pond (Science Applications International Corporations 1996). The Portsmouth X-625 and Y-12 water has pH values of 6.1–6.2 and 5.5–5.7 respectively. The alkalinity ranged from 83 to 85 mg/l in the X-625 water and from 300 to 500 mg/l in the Y-12 water. The dissolved oxygen varies from 0.2 to 5 mg/l and Fe^{2+} ranged from 0.3 to 0.6 mg/l in the X-625 water. The Portsmouth X-625 water is contaminated with TCE (150–200 μg/l) and the Y-12 water is contaminated with mainly uranium (~ 2 pCi/l). The X625 water has much less Ca, Na, and alkalinity than the Y-12 water, but the X-625 water has a slightly higher pH than the Y-12 water.

Chemical parameters monitored in the effluent following passage at the contaminated water through a reactive barrier included pH, dissolved oxygen, ferrous ion, alkalinity, and sulfate ion for field and laboratory observations. Effluent water from both Fe^0 filing and foam columns was collected directly into glass bottles or withdrawn by attaching a 5-ml glass syringe to prevent oxidation of dissolved iron in the treated water. Effluent pH was determined using an Orion model 920A pH meter equipped with an Orion combination electrode (Orion Inc., Boston, MA). Dissolved ferrous ion was determined using FerroVer iron reagent and sulfate concentration was determined with the methylene blue method (Hach DR/2000 Spectrophotometer Handbook, Loveland, CO). Dissolved oxygen was measured by using self-filling ampoules for colorimetric analysis from CHEMets (CHEMetrics, Inc., Calverton, VA). Alkalinity was determined by titration. The analytical precision for Fe^{2+}, SO_4^{2-}, and dissolved oxygen were ± 0.006, ± 0.003, and ± 0.002 mg/l respectively.

The immobilization of radionuclides by Fe^0 was conducted in the laboratory using either uranyl carbonate and pertechnetate solutions that were diluted with tap water or the uranium-contaminated Y-12 water (Table 3). Gamma activity of the ^{235}U and ^{95m}Tc isotopes in the solutions was determined using a high purity intrinsic germanium gamma-ray detector equipped with a Nuclear Data Model 6700 microprocessor programmed in 4096 channels (Cutshall and Larsen 1980). The counting error (2σ) was kept at $<2\%$ for all solutions.

The dechlorination of TCE by Fe^0 was determined in the laboratory using simulated groundwater that has a com-

Table 1
Reactive Fe^0 media used for treatment of contaminated waters

Reactive Fe^0 Medium	Size	Compositions	Mineralogy
Master Builder Fe^0 Filing	40 mesh	$\sim 95\%$ Fe^0 and carbon, and 5% other metals and silicon	Zero-valent iron (Fe^0), magnetite (Fe_3O_4)
Peerless Fe^0 filing	$+8$ to 50 mesh	$\sim 86\%$ Fe^0, 3–4% carbon, 3% silicon, and other metals	Zero-valent iron (Fe^0), magnetite (Fe_3O_4)
Cercona Fe^0 Foam	$+2$ to 8 mesh	92–94% Fe^0 balanced with aluminosilicate ($Al_2O_3{:}2SiO_2$)	Zero-valent iron (Fe^0), magnetite (Fe_3O_4), hercynite ($FeAl_2O_4$)

Table 2
Chemical composition in influent and effluent streams of the reactive barrier used in the field. *nd* Not determined

Parameter	X625 water, Portsmouth Gaseous Diffusion Plant, OH		GW-837 water, Y-12 Plant, Oak Ridge, TN	
	Influent[a]	Effluent[b]	Influent[c]	Effluent[b]
Dissolved oxygen (mg/l)	0.2–5	< 0.1	nd	nd
pH	6.1–6.2	6.9–7.3	5.6–5.7	6.9–7.5
Eh (mV)	400	–200– –400	420	0–200
Anions (mg/l)				
Alkalinity	83–85	50–270	300–500	50–100
Sulfate	400	150	461	461
Dissolved metals (mg/l)				
Calcium	21.3	nd	1681	nd
Fe(II)	0.3–0.6	55–125	14.3	17–250
Magnesium	13.3	nd	158	nd
Potassium	1.7	nd	42	nd
Sodium	18.7	nd	705	nd
Contaminants				
Uranium (pCi/l)	nd	nd	2.1–2.9	0.002–0.1
TCE (μg/l)	150–200	< 2	nd	nd

[a] Annual Report for 1997 Groundwater Monitoring Quarterly Sampling Results from Portsmouth Gaseous Diffusion Plant, Ohio, and Liang and others (1997)

[b] Values and value ranges of more than five samples analyzed

[c] Science Applications International Corporations (1996)

Table 3
Chemical composition in influent and effluent streams of the reactive barrier used in the laboratory. *DO* Dissolved oxygen

Parameter	Simulated ^{235}U-and ^{95m}Tc-contaminated water[b]		Y-12 water		Simulated TCE contaminated water[c]	
	influent	effluent	influent	effluent	influent	effluent
DO (mg/l)	4–5	< 0.01	3–5	< 0.01	4–5	< 0.01
pH	5.2	7.5–9.0	5.6–5.7	6.5–7.5	6.2	7.0–8.7
Eh (mV)	400	–50–400	420	0–400	430	0–200
Fe(II)	< 0.01	100–150	14.2	75–120	< 0.01	1.5–15
Contaminants						
Tc-95m (mg/l)	2.92E-9	BDL[d]				
U-235 (mg/l)	7–2500	< 25	2.1–2.9	BDL		
TCE (μg/l)					150–3200	< 2–750

[a] Values and value ranges of more than five samples analyzed

[b] Simulated water using tap water

[c] Simulated Portsmouth water

[d] Below detection limit

position similar to that of the Portsmouth Gaseous Diffusion Plant (Table 3). Samples for TCE and byproducts were collected from the influent and effluent lines using a 5.0-ml glass syringe. The aqueous samples were injected into a purge-and-trap concentrator (Teker 3000, Tekmar, Cincinnati, OH) and then analyzed for reaction byproducts by gas chromatography (GC) (HP-5890 Series II, Hewlett-Packard, Wilmington, DE) equipped with a flame ionization detector (FID) and a 0.53-mm capillary column (DB624, J&W Scientific, Folsom, CA). The method detection limit (MDL) for chlorinated organic compounds, as determined by the US EPA method (Environmental Protection Agency 1988), was 0.005 mg/l for TCE. For the field and laboratory study, columns used for groundwater treatment were opened and media used were sampled for morphological and mineralogical characterization. Portions of the column materials were used for the characterization of precipitated materials, corrosion products, and contaminant phases. Precipitates in the treated water were collected from treated water before and after aging by filtration with 0.45-μm Millipore filters. Precipitates on Fe^0 were isolated by sonification (~ 30 min) in acetone, filtered using a Millipore filter (< 0.45 μm), and used for mineralogical characterization. Mineralogical characterization of the precipitates was performed using (1) X-ray diffraction (XRD) using Scintag XDS 2000 diffractometer (Scintag Corporation, Sunnyvale, CA) at 45 kV, 40 mA, and (2) JEOL-JSM35CF scanning electron microscopy (SEM) with energy dispersive X-ray (EDX) analyzer (Tokyo, Japan).

Results and discussion

Iron hydroxide precipitation

A potential limitation of the reactive iron barrier is the deterioration of the Fe^0 materials by corrosion and subsequent precipitation of minerals that may cause cementation and decreased reactivity and permeability of the Fe^0 barrier. When the treatment column or reactor was opened after TCE dechlorination and radionuclide immobilization experiments in the laboratory and the field, Fe^0 filings and sand filters on the top of the columns were covered by crystalline and amorphous iron hydroxides. The SEM micrograph of Master Builder Fe^0 filings used for dechlorination at the Portsmouth site revealed that the Fe^0 was covered with Fe (hydr)oxides (Figs. 1a,b). The SEM with energy dispersive X-ray analysis of the Master Builder Fe^0 used for immobilization of radionu-

Fig. 1
Scanning electron micrograph of the reactive Fe^0 barrier used at (**a**) the Portsmouth site and at (**c**) the Y-12 site. EDX analyses of the reactive iron barrier used at (**b**) the Portsmouth site and at (**d**) the Y-12 site. (**e**) XRD analysis of amorphous iron oxides formed from Fe^0 filing used at the Portsmouth and Y-12 site

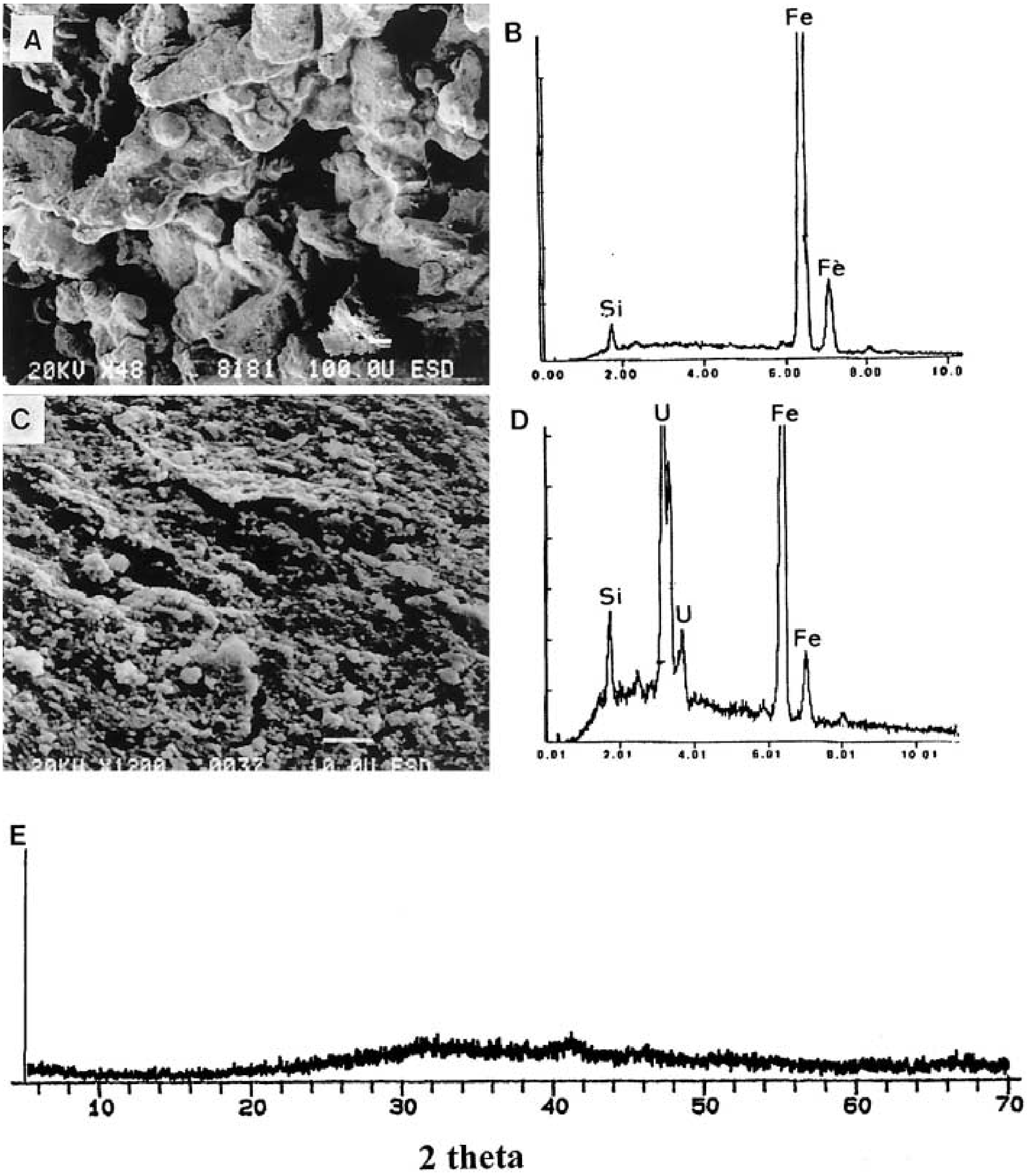

clides at the Y-12 site revealed that the Fe^0 was covered with Fe (hydr)oxides (Figs. 1c,d) and uranium precipitates (Fig. 1d). XRD analyses of the iron corrosion products recovered by sonification at the Portsmouth and Y-12 sites showed that corrosion products are X-ray amorphous (Fig. 1e).

Considerable concentration of Fe^{2+} by Fe^0 corrosion ($Fe^{2+} = 17–250$ mg/l) occurred when radionuclide-contaminated water from the Y-12 site and TCE-contaminated water from the X-625 water were treated with reactive iron barriers in the field (Table 2). The contaminants of concern (e.g. radionuclides and chlorinated organic compounds) are easily removed and dechlorinated from the contaminated water (Tables 2 and 3) by means of iron oxidation and electron and proton transfer. The Fe^0 corrosion is expected as the stability field of Fe^0 lies below the water redox line (Pourbaix 1973), indicating that Fe^0 should oxidize in the presence of water (reactions 1, 2) (Matheson and Tratnyek 1994).

$$Fe^0 = Fe^{2+} + 2e^- \quad \text{(iron oxidation)} \qquad (1)$$

$$Fe^0 + 2H_2O = Fe^{2+} + H_2 + 2OH^- \quad \text{(iron oxidation)} \qquad (2)$$

The corrosion of Fe and the pH increase leads to precipitation of $Fe(OH)_2$ (reactions 3).

$$Fe^0 + 2H_2O = Fe(OH)_2 + 2H^+ + 2e^- \quad \text{(precipitation of Fe hydroxide)} \qquad (3)$$

Oxidation of Fe^0 can proceed along several reaction pathways (Schwertmann and Cornell 1991). In reduced environments at low temperature, $Fe(OH)_2$ is stable, but is predicted thermodynamically to convert to either magnetite or intermediate products (green rusts). The SEM micrograph of the Master Builder Fe^0 filing used at Portsmouth revealed that the Fe hydroxide had a green rust mineral morphology, pseudo-hexagonal form (Fig. 2a), but XRD analyses could not confirm the presence of a green rust mineral because of the trace amounts of this mineral. Precipitates collected from the filtered effluents of the TCE dechlorination experiments using Portsmouth water and Peerless Fe^0 in the laboratory showed a platy, pseudo-hexagonal form as the Fe corrosion products (Fig. 2b). During reductive dechlorination, most of the chlorine is released as the chloride ion or combined with Fe^{2+} to precipitate out as amorphous Fe hydroxides $[Fe_3^{II}Fe^{III}(OH)_8Cl]$ and green rust I $[Fe_3^{II}Fe^{III}(OH)_8Cl]$. The SEM micrograph of Master Builder Fe^0 filing used at the Y-12 site also showed the presence of a green rust mineral morphology (Fig. 2c), and XRD analyses confirmed the presence of the hydrated sulfate form of green rust II (Table 4).

Uranium is easily susceptible to reduction and coprecipitation through oxidation of Fe^0 as shown in the following reactions (Roh and others 1996; Roh and others 2000b) because the uranyl cation (UO_2^{2+}) is redox sensitive in the natural environment:

$$Fe^0 + 1.5UO_2^{2+} + 6H^+ = Fe^{3+} + 1.5U^{4+} + 3H_2O \qquad (4)$$

Crystalline pyroaurite-like phases (green rust I, carbonate form) were formed by coprecipitation of reduced U with Fe eroded from a sponge-like Fe^0 foam under direct current during the remediation of the radionuclides, $^{235,238}U$ and ^{99}Tc, from contaminated waters (Fig. 2d, Table 4). Synthesis of pyroaurite-like phases through this electrochemical process is an effective approach to remediate contaminated aqueous solutions. The formation of a well-crystallized waste product is fortuitous because the solubility of crystalline products is expected to be much lower than that of an amorphous phase, thereby immobilizing the entrapped contaminants more effectively.

The green rusts (pseudo hexagonal form) and magnetite contain Fe^{2+} and Fe^{3+} in the structure whereas other Fe (hydr)oxides have only Fe^{3+}. The freshly-precipitated ferrihydrite reacts with excess Fe^{2+} in the system, which induces the hydrolysis of Fe^{2+} and leads to the formation of green rusts (Schwertmann and Cornell 1991; Hansen and others 1994). Green rust is a reductant capable of reducing heavy metals and radionuclides (Myneni and others 1997). Synthetic or natural materials of similar crystal structure are likely able to reduce nitrate and heavy metals under abiotic conditions, although these reactions are generally quite slow (Hansen and others 1996).

Iron metal can be transformed into green rusts such as $[Fe_4(OH)_8Cl\ nH_2O]$, $[Fe_6(OH)_{12}][CO_3\ nH_2O]$, and $[Fe_7(OH)_{18}SO_4\ nH_2O]$ in moderately neutral solutions ($6.5 < pH < 8.0$) and is passivated by Fe oxides (Odziemkowski and others 1998) or transformed into hydrated forms of ferrous/ferric iron oxides, as shown in the following reactions:

$$3Fe(OH)_2(s) = Fe_3O_4(s) + H_2(g) + 2H_2O + 2e^- \quad \text{(transformation into magnetite)} \qquad (5)$$

$$4Fe(OH)_2(s) + Cl^- = Fe_3^{II}Fe^{III}(OH)_8Cl + e^- \quad \text{(transformation into green rust I)} \qquad (6)$$

$$6Fe(OH)_2(s) + CO_3^{2-} + 2H_2O = [Fe_4^{II}Fe_2^{III}(OH)_{12}][CO_3 \cdot 2H_2O] + 2e^- \quad \text{(transformation into green rust I)} \qquad (7)$$

$$6Fe(OH)_2(s) + SO_4^{2-} + 2H_2O = [Fe_4^{II}Fe_2^{III}(OH)_{12}][SO_4 \cdot 2H_2O] + 2e^- \quad \text{(transformation into green rust II)} \qquad (8)$$

Green rusts as an intermediate product during the hydrolytic oxidation of Fe^{2+} solutions often transform to FeOOH (Olowe and Genin 1991). Green rusts convert to goethite (α–FeOOH), lepidocrocite (γ–FeOOH), maghemite (Fe_2O_3), or magnetite (Fe_3O_4), depending on the rate of oxidation and dehydration (Myneni and others 1997). SEM and XRD analyses of the Peerless and Master Builder Fe^0 filings used at the Portsmouth site revealed the presence of lepidocrocite (γ–FeOOH) (Table 4) and goethite (α–FeOOH) with irregular platy- or spherical-shaped amorphous iron hydroxides (Fig. 2f). The crystalline Fe minerals are believed to have been transformed from the amorphous Fe hydroxides, but when is not known. Dome-shaped Fe (hydr)oxide crusts were commonly observed on the Master Builder Fe^0 filing samples used at Portsmouth site (Fig. 2e,f), whereas lepidocrocite and goethite were predominant as precipitates on the Master Builder Fe^0 filing used at the Y-12 site. X-ray dif-

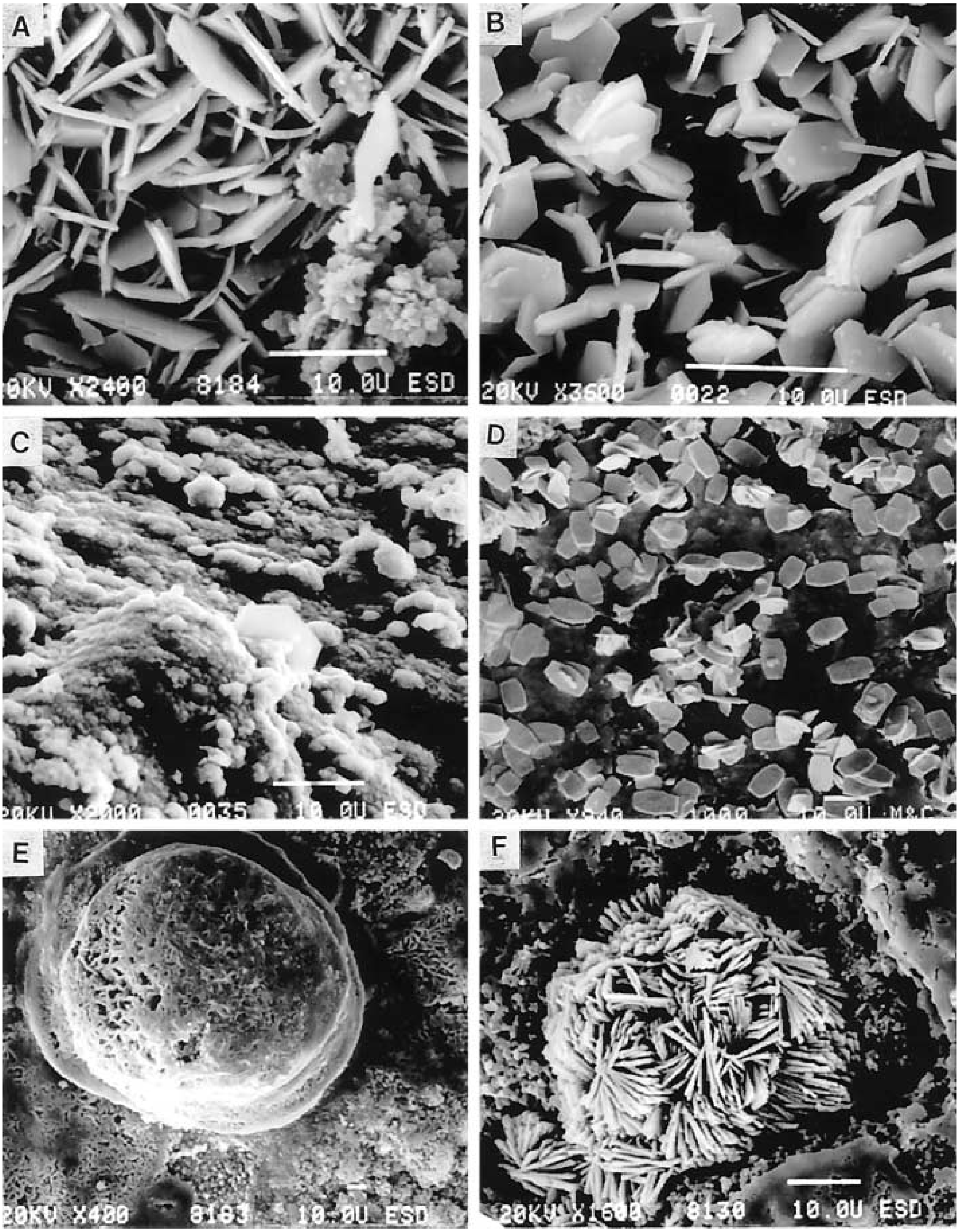

Fig. 2
Scanning electron micrograph: (**a**) green rust formed from Peerless Fe^0 filing used at the Portsmouth site, (**b**) green rust formed from Peerless Fe^0 filing during electrochemical dechlorination of TCE, (**c**) green rust formed from Master Builder Fe^0 filing used at the Y-12 site, and (**d**) green rust formed from Cercona Fe^0 foam during electrochemical immobilization of radionuclides. Scanning electron micrograph of (**e**) iron hydroxide formation from dome-shaped iron (hydr)oxides, (**f**) goethite formation with micropore

fraction analyses confirmed the presence of iron hydroxide, including goethite, at the Portsmouth and Y-12 site (Table 4).

Iron metal is predicted to transform into Fe hydroxide (FeOOH) in the presence of alkaline solutions ($pH > 8.0$) (Olowe and Genin 1991; Schwertmann and Cornell 1991; Drissi and others 1995; Genin and others 1996; Refait and others 1997; Simon and others 1997) as shown in the following reaction:

Table 4
Summary of the reactive iron barrier experiments in the field and laboratory

Contaminated waters	Operation period	Reactive Fe^0 media	Flow rate	Mineralogy
Ex situ field study				
X-625 water, Portsmouth site, Portsmouth, OH	6 months	Peerless Fe^0 filing, Master Builder Fe^0 filing	11.34 ml/min	Amorphous Fe (hydr)oxides, goethite, magnetite, akageneite, lepidocrocite, green rust I (chloride form), iron sulfide, sulfur
GW-837 water, Y-12 site, Oak Ridge, TN	2 months	Master Builder Fe^0 filing	2 ml/min	Amorphous Fe (hydr)oxides, goethite, lepidocrocite, green rust I (carbonate form), green rust II (sulfate form), magnetite, akageneite, aragonite, calcite, siderite
Laboratory study without direct current				
Simulated Portsmouth TCE-contaminated water	3 days	Peerless Fe^0 filing, Master Builder Fe^0 filing	4 ml/min	Amorphous Fe (hydr)oxides, green rust I (chloride form)
U- and Tc-contaminated water simulated with tap water	8 h	Cercona Fe^0 foam	6.2 ml/min	Amorphous Fe (hydr)oxides
GW-837 water, Y-12 Site, Oak Ridge, TN	3 days	Peerless Fe^0 filing	2 ml/min	Amorphous Fe (hydr)oxides, calcite, siderite
Laboratory study with direct current				
TCE-contaminated water simulated with tap water	3 days	Peerless Fe^0 filing	4 ml/min	Amorphous Fe (hydr)oxides, green rust I (chloride form)
U- and Tc-contaminated water simulated with tap water	8 h	Cercona Fe^0 foam	6.2 ml/min	Amorphous Fe (hydr)oxides, green rust I (carbonate form)
GW-837 water, Y-12 site, Oak Ridge, TN	3 days	Peerless Fe^0 filing	2 ml/min	Amorphous Fe (hydr)oxides, green rust II (sulfate form)

$$Fe(OH)_2(s) = FeO(OH) + H^+ + e^- \quad \text{(transformation into iron hydroxides)} \qquad (9)$$

If this reaction occurs on the surface of the iron barrier, these surface coating materials could limit access of the contaminants to the Fe^0 surface for reductive dechlorination and coprecipitation. The precipitates also block the pore spaces between iron particles. This may result in the appearance of daughter products of incomplete dechlorination and unreacted radionuclides appearing in the effluent after the reaction period of the treatment.

Calcium carbonate, iron carbonate, and iron sulfide precipitation

The chemical composition of the contaminated groundwater controls the mineralogy of the precipitates in the reactive iron barrier. The alkalinity decrease in the Y-12 site water (Table 2) suggests the precipitation of ferrous carbonate (siderite) and Ca-carbonate (aragonite and calcite). These geochemical changes can result in precipitation on the reactant surfaces. Waters high in carbonate, such as the Y-12 site, result in a significant buildup of calcite (Fig. 3a) and siderite (Fig. 3c, Table 4). Waters high in carbonate may result in significant buildup of calcite ($CaCO_3$) or siderite ($FeCO_3$) (Blengino and others 1995). Depending on the chemical composition of the groundwater, such minerals including aragonite have been precipitated (Fig. 3b, Table 4). The presence of sulfate and magnesium in the influent water at the Y-12 site (Table 2) promoted the formation of aragonite rather than calcite (Berner 1975). The carbonate coatings on the reactive Fe^0 surface could prevent adsorption and precipitation of the reducible radionuclides from the contaminated water, especially in limestone aquifers such as the Y-12 site (Science Applications International Corporations 1996).

Iron corrosion produces OH^- ions that increase pH (Tables 2 and 3) and react with dissolved carbonic acid and bicarbonate species in the groundwater to produce carbonate ions:

$$H_2CO_3^0 + 2OH^- = CO_3^{2-} + 2H_2O(l) \qquad (10)$$

$$HCO_3^- + OH^- = CO_3^{2-} + H_2O(l) \qquad (11)$$

Fig. 3
Scanning electron micrograph of (**a**) calcite and (**b**) aragonite formed on Fe^0 filing used at the Y-12 site, and (**c**) XRD analysis of siderite (s) formed from Fe^0 filing used at the Y-12 site iron barrier. Scanning electron micrograph of (**d**) mackinawite and (**e**) sulfur formed on Fe^0 filing used at the Portsmouth site, and (**f**) XRD analysis of mackinawite (*m*) formed from Fe^0 filing used at the Portsmouth site

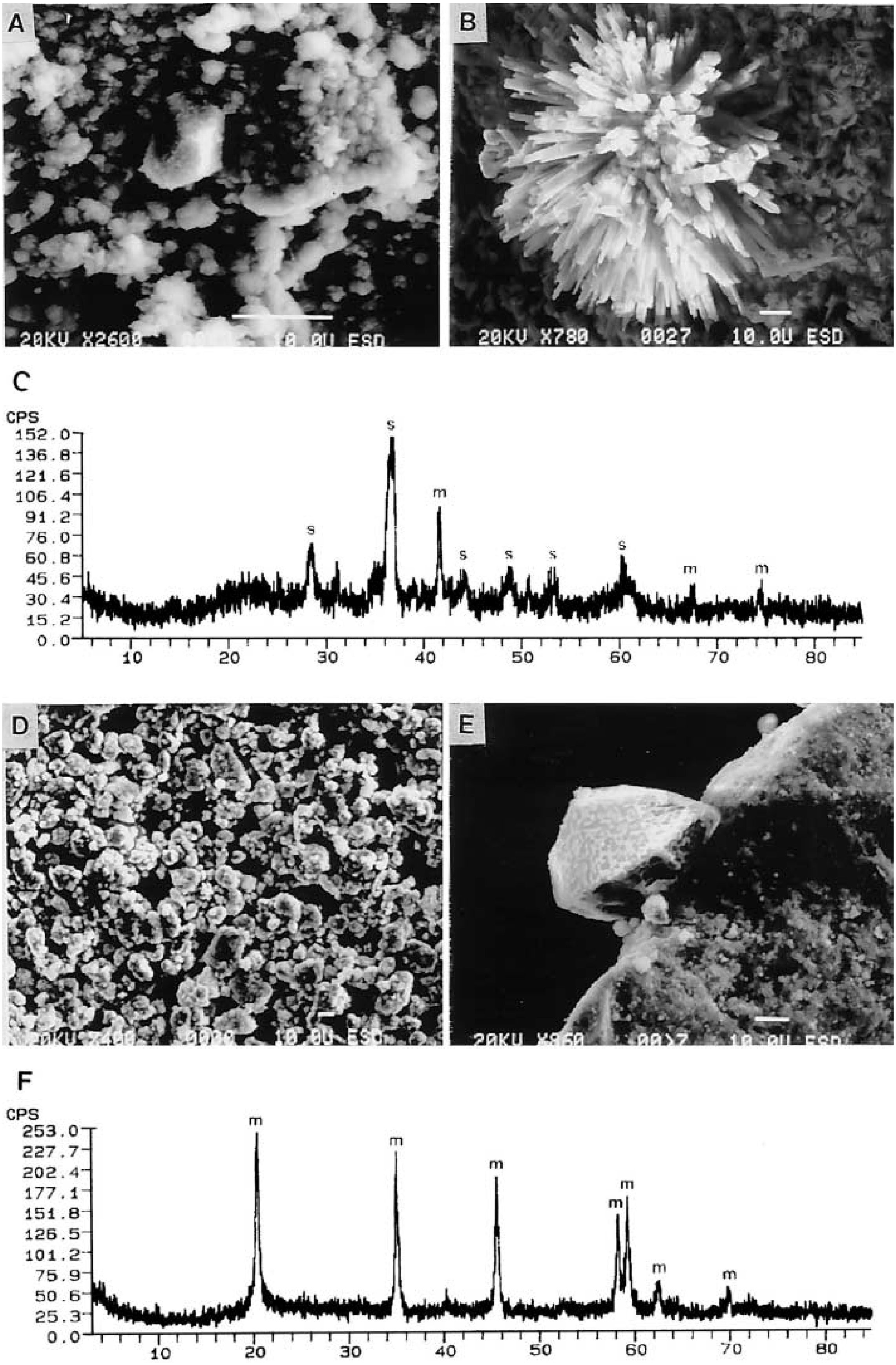
A
20KV X2600
10.0U ESD
B
20KV X780 0027 10.0U ESD
C
CPS
152.0
136.8
121.6
106.4
91.2
76.0
60.8
45.6
30.4
15.2
0.0
s
m
10
20
30
40
50
60
70
80
D
10.0U ESD
E
20KV
10.0U ESD
F
CPS
253.0
227.7
202.4
177.1
151.8
126.5
101.2
75.9
50.6
25.3
0.0
m
10
20
30
40
50
60
70
80

Buildup of carbonate ions eventually results in the precipitation of carbonate solid species:

$$Ca^{2+}(aq) + CO_3^{2-} = CaCO_3(s) \quad (12)$$

$$Ca^{2+}(aq) + HCO_3^-(aq) = CaCO_3(s) + H^+ \quad (13)$$

$$Fe^{2+}(aq) + CO_3^{2-} = FeCO_3(s) \quad (14)$$

$$Fe^{2+}(aq) + HCO_3^-(aq) = FeCO_3(s) + H^+ \quad (15)$$

Both Fe^0 filings used at the Portsmouth site were dark in color and did not have the metallic sheen of the unused materials. X-ray diffraction analyses of the coated precipitates on the Fe filings (Fig. 3f) separated by sonification showed that iron sulfide (mackinawite, FeS_{1-x}) precipitated in the Fe^0 filing during the TCE-contaminated groundwater treatment. The decrease in sulfate concentration at the Portsmouth site (Table 2) is attributed to microbial activity of the sulfate-reducing bacteria because iron sulfide was formed as a result of microbial reduction of SO_4^{2-} (Gu and others 1999). The occurrence of sulfate-reducing bacteria can thereby affect the mineralogy of the precipitates in the reactive iron barrier. Sulfate-reducing bacteria were detected in the water samples collected from the treatment trains and in the iron filing used from the canisters at the Portsmouth site (Liang and others 1997). Therefore, Fe sulfide, mackinawite, may be precipitated (Figs. 3d,f) via the occurrence of sulfate-reducing bacteria and Fe oxidation (McNeil and Little 1990). Pyramidal sulfur crystals (Fig. 3e) were formed through sulfate reduction by the action of sulfur-forming bacteria as reported by Hurlbut and Klein (1985). The sulfate-reducing bacteria normally influence the corrosion of metals (Hamilton 1985; Lee and others 1993):

$$SO_4^{2-} + 8H^+ + 8e^- = S^{2-} + 4H_2O \quad (16)$$

(cathodic depolarization reaction by sulfate-reducing bacteria)

$$4Fe^0 + SO_4^{2-} + 4H_2O = FeS + 3Fe(OH)_2 + 2OH^- \quad (17)$$

(Fe sulfide precipitation)

A potential negative consequence of bacteria is biofouling because the proliferation of bacteria in an improperly designed reactive barrier could reduce the hydraulic conductivity of the barrier, thereby hindering the flow of groundwater through it (Weathers and others 1997).

Effect of precipitates on iron wall performance

It has been proven that Fe oxidation is one of the main mechanisms of reductive dechlorination of TCE and immobilization of reducible toxic metals and radionuclides (Matheson and Tratnyek 1994; Roh and others 2000a,b). However, the role of the Fe hydroxide surface film formed by the hydrolysis of the oxidized Fe on the dechlorination rate of TCE and coprecipitation rate of the heavy metals and radionuclides are not very well understood. There is uncertainty over how to incorporate the kinetics of the oxide film growth on the metal surface with the kinetics of dechlorination, adsorption, and coprecipitation. The long-term performance is still an issue because iron oxidation will be slowed with time as a result of the passivation of the surfaces by increasing thickness of inorganic surface layers.

Flow through the reactive Fe^0 barrier at the Portsmouth X-625 facility was relatively stable during the first month [3 gpm (gallons per minute)], but flow through the Master Builder Fe^0 filing train started to decrease from <1 to 0.3 gpm after ~2 months operation (Liang and others 1997). Flow through the Peerless Fe^0 treatment train was relatively stable in comparison with that of the Master Builder Fe^0 treatment train because there appears to be a decreasing trend in flow-through after ~5 months operation in the Master Builder Fe^0 treatment train (Liang and others 1997). The apparent decrease in flow rate is attributed to the precipitation of Fe (hydr)oxides, sulfides and carbonates, thereby reducing pore spaces available for water flow (Figs. 1 and 2; Table 4).

According to Liang and others (1997), at the system start-up phase with both Fe^0 barriers at the Portsmouth site, TCE removal was rapid: the half-life of TCE dechlorination has <19 min for Peerless Fe^0 filing and 10 min for Master Builder Fe^0 filing until approximately 45 pore volumes of water were treated. The half-life of TCE dechlorination in Peerless Fe^0 filing trains more than doubled (43.4 min) when 144 to 562 pore volumes of water were treated. The half-life of TCE dechlorination in Master Builder Fe^0 filing increased to 43.5 min after 326 pore volumes of water were treated. The changes in degradation characteristics with time are attributed to (1) reduction in Fe surface reactivity caused by passivation of Fe^0 by precipitates, including Fe (hydr)oxides and Fe sulfides (Table 4), and (2) alternation of flow paths through Fe filings as a result of precipitation and cementation (Fig. 4). Flow rates at Y-12 sites were not changed for the 2-month trial and there is no dissolved uranium detected in the treated water (Science Applications International Corporations 1998). However, the flow rates and effectiveness of the reactive iron barrier at Y-12 are expected to change with time because of expected calcium carbonate and iron (hydr)oxides formation.

The effect of these precipitates in reactive barrier over the lifetime of an in situ field installation is not fully understood, but column clogging in an ex situ field operation and lab studies has been observed. Thus, successful application of this reactive barrier requires a detailed characterization of the contaminants, groundwater chemistry, groundwater flux, and subsurface geology. Periodic sampling of the influent and effluent for the contaminants of interests, plus monitoring of flow rates and system back-pressure are needed to evaluate the system operation. Studies for ways of controlling Fe corrosion and precipitation are needed because the discharge of soluble Fe from the permeable reactive barrier may affect the hydraulic conductivity of the soil and sediment downgradient of the treatment system.

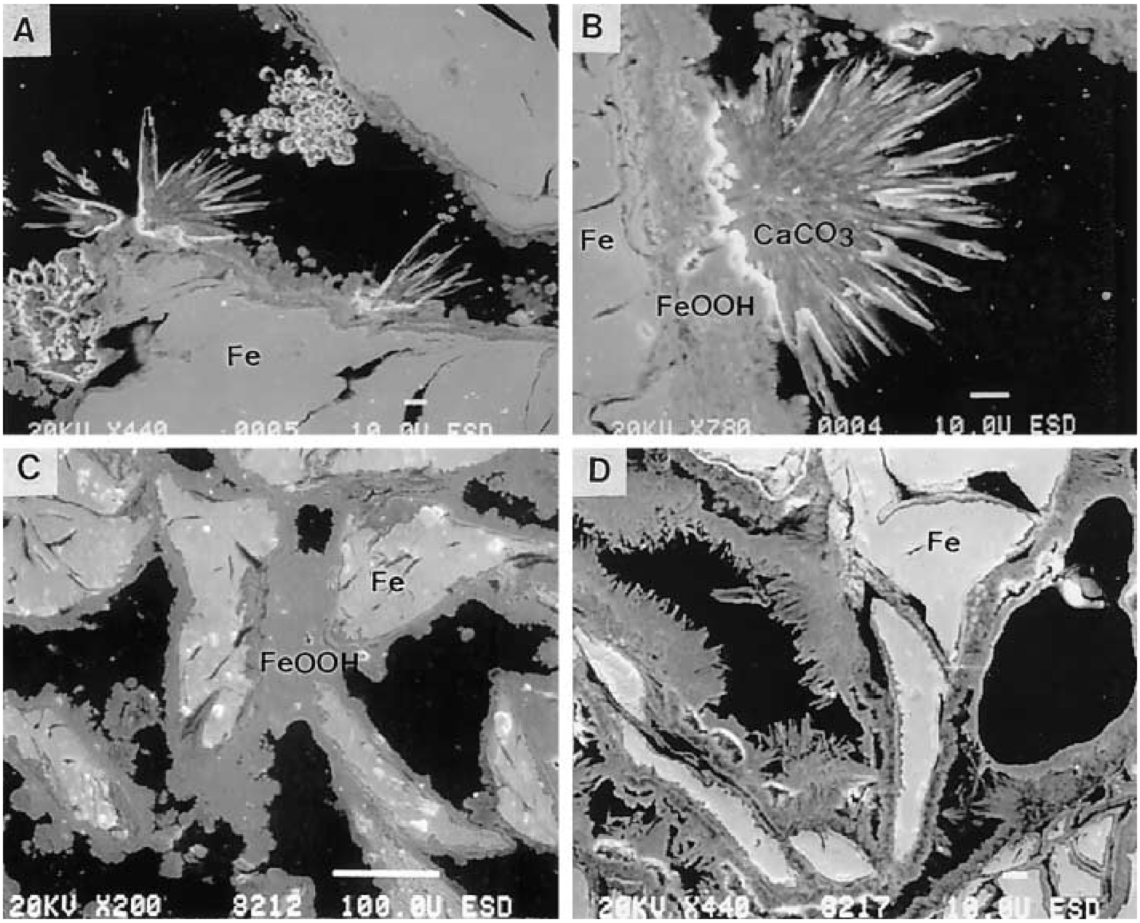

Fig. 4
(**a,b**) Polished cross section showing surface coating of iron hydroxides and aragonite on Fe^0 filings used at the Y-12 site. Polished cross section showing surface coating of surface coating on (**c**) Peerless Fe^0 filings and (**d**) Master Builder Fe^0 filings used at the Portsmouth site

Conclusions

The principal corrosion products of Fe in reactive Fe^0 media are amorphous iron (hydr)oxides, intermediate products (green rusts), and hydrated forms of ferric oxides such as akaganeite (β–FeOOH), goethite (α–FeOOH), lepidocrocite (γ–FeOOH). Other minerals such as calcite, aragonite, siderite, mackinawite, and elemental sulfur also precipitated on the surface of reactive media. The formation of a well-crystallized, U-containing green rust phases is fortuitous because the solubility of crystalline products are expected to be much lower than that of an amorphous (Fe oxide) phase, thereby immobilizing the entrapped contaminants more effectively. However, the precipitates including iron oxides, carbonates, and iron sulfides in reactive iron barriers block the pore spaces between iron particles. This may result in the appearance of daughter products of incomplete dechlorination and unreacted radionuclides appearing in the effluent after the reaction period of the treatment.

Many factors contribute to the mineralogy of the precipitates including (1) contaminants in the groundwater; (2) chemical composition of the groundwater; and (3) occurrence of sulfate-reducing bacteria. The observed morphology of the reactor bed fragments indicates that the reduction of flow rate and reactivity was caused by the buildup of precipitates on Fe^0 surfaces. Thus, successful application of this reactive barrier requires a detailed characterization of the contaminants, groundwater chemistry, and subsurface geology. In addition to periodic sampling of the influent and effluent for the contaminants of interests, monitoring of flow rates would also be needed to evaluate system operation.

Acknowledgments This research was supported by Oak Ridge National Laboratory, which is managed by Lockheed Martin Energy Research Corp., under contract DE-AC05-96OR22464 with the US Department of Energy. Environmental sciences division publication # 4992.

References

Berner RA (1975) The role of magnesium in the crystal growth of calcite and aragonite from sea water. Geochim Cosmochim Acta 38:489–504

Blengino JM, Keddam M, Labbe TP, Lobbiola L (1995) Physico-chemical characterization of corrosion layers formed on iron in a sodium carbonate–bicarbonate containing environments. Corrosion Sci 37:621–643

Cantrell KJ, Kaplan DI, Wiestsma, TW (1995) Zero-valent iron for the in situ remediation of selected metals in groundwater. J Hazard Materials 42:201–212

Cutshall NH, Larsen IL (1980) BGSUB and BGFIX: Fortran programs to correct Ge(Li) gamma-ray spectra for photopeaks from radionuclides in background. ORNL/TM-7051, Oak Ridge National Laboratory, Oak Ridge, Tennessee.

Drissi SH, Refait Ph, Abdelmoula M, Genin JMR (1995) The preparation and thermodynamic properties of Fe(II)–Fe(III) hydroxide-carbonate (green rust 1); Pourbaix diagram of iron in carbonate-containing aqueous media. Corrosion Sci 37:2025–2041

Environmental Protection Agency (1988) US EPA methods for the determination of organic compounds in drinking water: method 502.2, Revision 2.0, EPA-600/4-88/039, US Environmental Protection Agency, Cincinnati, Ohio

Environmental Protection Agency (1996) A citizen's guide to treatment walls. United States Environmental Protection Agency. EPA 542-F-96-001

Genin JMR, Olowe AA, Refait, PH (1996) On the stoichiometry and Pourbaix diagram of Fe(II)–Fe(III) hydroxy-sulfate or sulfate containing green rust, 2: An electrochemical and Mössbauer spectroscopy study. Corrosion Sci 38:1751–1762

Gillham RW, O'Hanneisin SF (1994) Enhanced degradation of halogenated aliphatics by zero-valent iron. Ground Water 32:958–967

Gu B, Phelps TJ, Liang J, Dickery MJ, Roh Y, Kinsall BL, Palumbo AV, Jacobs GK (1999) Biogeochemical dynamics in zero-valent iron columns: implications for permeable reactive barriers. Environ Sci Technol 33:2170–2177

Haggerty GM, Bowman, RS (1994) Sorption of chromate and other inorganic anions by organo-zeolite. Environ Sci Technol 28:452–458

Hamilton WA (1985) Sulfate-reducing bacteria and anaerobic corrosion. Ann Rev Microbiol 39:195–217

Hansen HCB, Borggaard OK, Sorensen J (1994) Evaluation of the free energy of formation of Fe(II)–Fe(III) hydroxide-sulfate (green rust) and its reduction of nitrite. Geochim Cosmochim Acta 58:2599–2608

Hansen HCB, Koch CB, Nancke-Krogh H, Borggaard OK, Sorensen, J (1996) Abiotic nitrate reduction to ammonium: key role of green rust. Environ Sci Technol 30:2053

Hurlbut CS Jr, Klein C (1985) Manual of mineralogy, 20th edn. Wiley, New York

Lee SY, Bondietti EA (1983) Removing uranium from drinking water by metal hydroxide and anion exchange resin. Am Water Works Assoc 75:537–540

Lee W, Lewandowski Z, Okabe S, Characklis WG, Avci R (1993a) Corrosion of mild-steel underneath aerobic biofilms containing sulfate reducing bacteria. Part I: at low dissolved oxygen concentration. Biofouling 7:197–216

Lee W, Lewandowski Z, Okabe S, Characklis WG, Avci R (1993b) Corrosion of mild-steel underneath aerobic biofilms containing sulfate reducing bacteria. Part II: at high dissolved oxygen concentration. Biofouling 7:217–239

Liang L, West OR, Korte NE, Goodlaxson JD, Pickering DA, Zutman JL, Anderson FA, Welch CW, Pelfrey MJ, Dickery MJ (1997) The X-625 groundwater treatment facility: a field-scale test of trichloroethene dechlorination using iron filing for the X-120/X-749 groundwater plume. ORNL/TM-13410. Oak Ridge National Laboratory. Oak Ridge, Tennessee

Matheson LJ, Tratnyek PG (1994) Reductive dehalogenation of chlorinated methanes by iron metal. Environ Sci Technol 28:2045–2053

McNeil MB, Little, BJ (1990) Mackinawite formation during microbial corrosion. Corrosion 46:599–600

Morrison SJ, Spangler RR (1993) Chemical barriers for controlling groundwater contamination. Environ Prog 12:175–181

Myneni SCB, Tokunaga TK, Brown, GE (1997) Abiotic selenium redox transformation in the presence of Fe(II,III) oxides. Science 278:1106–1109

Odziemkowski MS, Schuhmacher TT, Gillham RW, Reardon EJ (1998) Mechanism of oxide film formation on iron in simulating groundwater solutions: raman spectroscopic studies. Corrosion Sci 40:371–389

Olowe AA, Genin JMR (1991) The mechanism of oxidation of ferrous hydroxide in sulfated aqueous media: importance of the initial ratio of the reactants. Corrosion Sci 32:965–984

Orth WS, Gillham RW (1996) Dechlorination of trichloroethene in aqueous solution using Fe^0. Environ Sci Technol 30:66–71

Pourbaix M (1973) Lectures on electrochemical corrosion. Plenum Press, New York

Powell RM, Puls RW, Hightower SK, Sabatini DA (1995) Coupled iron corrosion and chromate reduction: mechanisms for subsurface remediation. Environ Sci Technol 29:1913–1922

Refait Ph, Drissi SH, Pytkiewicz J (1997) The anionic species competition in iron aqueous corrosion: role of various green rust compounds. Corrosion Sci 39:1699–1710

Roh Y, Lee SY, Elless MP (1996) Electroremediation of uranium and technetium contaminated waters. Extended Abstract. Annual Meeting of the Chemical Society, I&EC Division, Emerging Technologies in Hazardous Waste Management VIII, 9–12 Sept 1996. Birmingham, Alabama, pp 582–585

Roh Y, Lee SY, Elless MP, Moon, HS (2000a) Electro-enhanced remediation of trichloroethene-contaminated groundwater using zero-valent iron. J Environ Sci Health, Part A. 35(7) pp 1061–1076

Roh Y, Lee SY, Elless MP, Cho, KS (2000b) Electro-enhanced remediation of radionuclide-contaminated groundwater using zero-valent iron. J Environ Sci Health, Part A. 35(7) pp 1043–1059

Schwertmann U, Cornell RM (1991) Iron oxides in the laboratory. VCH Publishers, New York

Science Applications International Corporations (1996) Phase I report on the Bear Creek Valley treatability study, Oak Ridge Y-12 Plant, Oak Ridge, Tennessee, Lockheed Martin Energy System, Inc. Y/ER-285

Science Applications International Corporations (1998) Bear Creek Valley treatability study. Phase II technical memoranda, Oak Ridge Y-12 Plant, Oak Ridge, Tennessee. Bechtel Jacobs Company. BJC/OR-2

Simon L, Genin JMR, Refait Ph (1997) Stand free enthalpy of formation of Fe(II)–Fe(III) hydroxysulphite green rust one and its oxidation into hydroxysulfate green rust two. Corrosion Sci 39:1673–1685

Weathers LJ, Parkin GF, Alvarez, PJ (1997) Utilization of cathodic hydrogen as electron donor for chloroform cometabolism by a mixed methanogenic culture. Environ Sci Technol 31:880–885